Journal of Non-Crystalline Solids: X 8 (2020) 100051

Contents lists available at ScienceDirect

Journal of Non-Crystalline Solids: X

journal homepage: www.journals.elsevier.com/journal-of-non-crystalline-solids-x

Rejuvenation through plastic deformation of a La-based metallic glass measured by fast-scanning calorimetry

C.M. Meylan[a,*], J. Orava[b], A.L. Greer[a,*]

[a] Department of Materials Science & Metallurgy, University of Cambridge, 27 Charles Babbage Road, Cambridge CB3 0FS, UK
[b] IFW Dresden, Institute for Complex Materials, Helmholtzstraße 20, Dresden 01069, Germany

ARTICLE INFO

Keywords:
Fictive temperature
Metallic glass
Plastic deformation
Rejuvenation
Relaxation
Ultra-fast scanning calorimetry

ABSTRACT

We explore the glassy states achievable after a metallic glass is formed on liquid quenching. Samples of $La_{55}Al_{25}Ni_{20}$ (at.%) metallic glass (rod and ribbon) are studied. The extent of structural relaxation at room temperature is characterized for this low-glass-transition temperature glass. Plastic deformation (uniaxial compression) rejuvenates the glass to states of higher enthalpy characteristic of glass formation at high cooling rate. Deformation increases the heterogeneity of the glass, widening the spectrum of relaxation times. The extent of rejuvenation in samples of low aspect ratio is compared with that under conditions of high constraint in notched samples. The deformation-induced rejuvenation is particularly susceptible to reduction on subsequent ageing. Fast-scanning calorimetry is useful in characterizing the dynamics of structural relaxation. The shadow glass transition is more evident on fast heating, and is observed in this glass for the first time. A new excess exothermic effect is observed before the glass transition.

1. Introduction

A given metallic glass (MG) composition can show a range of energy states. *Relaxation* (*ageing*) to states of lower enthalpy can cause embrittlement, so in pursuit of better plasticity and toughness there is an interest in *rejuvenation* to reach states of higher enthalpy [1]. Plastic deformation is one of the more straightforward methods by which rejuvenation can be achieved. The degree of rejuvenation, quantified as the increase in the heat of relaxation (ΔH_{rel}) on heating a MG up to the glass-transition temperature T_g, scales linearly with the imposed plastic strain ε_p [2–4].

In MG ribbons rolled at room temperature (RT), the stored energy (increase in enthalpy) resulting from deformation was found to be ~4% of the mechanical work done (WD) [3]. In deformation of amorphous polymers, in contrast, the stored energy is 30–60% of the WD [5]. The energy storage in MGs is low because at RT plastic flow is localized in thin (~10 to ~20 nm) shear bands (SBs) that occupy only a low volume fraction (10^{-4} to 10^{-1}) of the glass [6]. In these SBs, the effects of deformation must saturate at shear offsets that are much smaller than sample dimensions, and the stored energy may relax downwards due to local heating. The stored energy may relax downwards also due to shear-band induced intermixing causing local change in the composition of the shear bands [7].

The highest stored energy for plastic deformation of a MG is reported at the notch root in a circumferentially notched rod subjected to compression along its axis [8]; averaging over the deformed volume in the sample, the stored energy is ~29% of the WD, a fraction reaching the lower end of the range for polymers. In the constraint of the notched specimen, rejuvenation is favoured: (i) by flow of the MG that is homogeneous (not localized in SBs); and (ii) by the component of hydrostatic compression in the stress state. Under deformation, the amount of rejuvenation that can be achieved reflects a balance between damage and relaxation [1]; the degree of hydrostatic compression in the notched cylinder seems to completely suppress relaxation, suggesting that the system may be over-constrained [8].

The high fraction of work done that remains as stored energy by deformation of notched samples is attractive [8], but the sample preparation is not straightforward and may be especially difficult for MG compositions that are more brittle than that used so far. The present work explores whether some or all of such enhanced rejuvenation could be achieved with less constraint, specifically by uniaxial compression of disc samples of low aspect ratio (height:diameter).

This study is based on a lanthanum-based MG capable of being formed in bulk; this family of MGs is of interest for: showing rejuvenation by other methods [9], RT ageing effects [10], pronounced β relaxation [11,12], and a possible fragile-to-strong crossover in the liquid state [13]. Extensive studies have shown that much can be learnt about structural relaxation dynamics in glasses by conventional

* Corresponding authors at: University of Cambridge, Department of Materials Science & Metallurgy, 27 Charles Babbage Road, Cambridge CB3 0FS, UK.
E-mail addresses: cmg63@cam.ac.uk (C.M. Meylan), j.orava@ifw-dresden.de (J. Orava), alg13@cam.ac.uk (A.L. Greer).

https://doi.org/10.1016/j.nocx.2020.100051
Received 21 February 2020; Received in revised form 2 June 2020; Accepted 3 June 2020
Available online 06 June 2020

differential scanning calorimetry (CDSC) of samples that are *hyperquenched* (i.e. have been formed at cooling rates much higher than the standard rate of 0.33 K s^{-1}) and then annealed [13–15]. This approach has been applied to the particular MG used in the present work [14]. We extend such studies to the much higher heating rates obtainable with fast (flash) differential scanning calorimetry (FDSC) which allows changes in effective specific heat to be detected with much greater sensitivity.

We characterize the MG states in terms of not only stored energy but also *fictive temperature* T_f [16]. On simple quenching at a given rate, the liquid-to-glass transition occurs at a given temperature and gives a MG with particular enthalpy $H(T)$. On faster cooling, the glass transition occurs at higher temperature and the resulting MG has higher $H(T)$. The different possible glassy states can be characterized by T_f, defined as the temperature at which the enthalpy-temperature lines of the glass and of the supercooled liquid intersect; T_f can be determined calorimetrically through the equal-area construction [16] and, unlike T_g determined on heating, its value is independent of heating rate. Any MG sample, however treated (e.g. annealed or deformed), can similarly be described in terms of its T_f, which is the temperature at which the glass transition would have occurred on cooling if an energetically equivalent MG were formed by quenching, and this allows the effective cooling rate to be calculated [8]. A question explored in previous work [17], and revisited in the present work, is the extent to which T_f is an adequate description of a given glassy state.

2. Experimental methods

The samples were obtained from the Institute of Physics, Chinese Academy of Sciences, Beijing, where master alloys of nominal composition $La_{55}Al_{25}Ni_{20}$ (at.%) were prepared by arc-melting 3–4 N pure elements. Bulk metallic glass (BMG) rods, diameter 2.0 mm, length up to 80 mm, were made by induction-melting and suction-casting, under Ti-gettered argon atmosphere, into water-cooled Cu-moulds. Glassy ribbons, ~45 μm thick, were melt-spun, under argon atmosphere, on a copper wheel at 4000 r.p.m.

A rod was cut into 250–400 μm thick discs, which were compressed (Tinius Olsen H25K-S UTM) along the rod axis at RT at a displacement rate of 0.015 mm min^{-1}. Ultimate loads of 6, 8 and 20 kN were applied to deform the samples by 30, 37 and 53%, respectively. Greater deformations (55, 63, 71, 83, 85%) were achieved by cutting the discs to reduce the area of the faces, thereby increasing the applied stress for a given load. The height:diameter ratio of the samples was always below 0.4. The degree of deformation (plastic strain ε_p) is defined as $(d_{init} - d_{def})/d_{init}$, where d_{init} and d_{def} are the sample heights (disc thickness) measured before and after compression. Samples were analysed by FDSC either < 6 h or < 30 h after deformation. Due to relaxation on storage at RT, this range of time could affect the measured values of stored energy, but the effect is less than the sample-to-sample variation for a given degree of deformation.

For FDSC, a Mettler Toledo Flash DSC1 was operated with UFS 1 sensors and purged with nitrogen at 30 ml min^{-1}. Disc samples were polished from both faces down to 20 μm thickness, then cut by a scalpel into $(\sim 0.1\ mm)^2$ pieces. The change in ΔH_{rel} was measured by heating from 303 K to 793 K at 100 K s^{-1}, holding isothermally for 0.1 s, then cooling to 303 K at the same rate. A second heating run provided a baseline. Four to 10 samples were measured per sample condition. After baseline subtraction, the FDSC curves were scaled and shifted to match measured specific-heat values [18] of 22.7 J mol^{-1} K^{-1} at 350 K (in the crystal, assumed here to apply for the glass) and 37.6 J mol^{-1} K^{-1} at 550 K (in the supercooled liquid). By this scaling, the changes in ΔH_{rel} are determined absolutely without the need to know sample masses (~1 μg), which are not straightforward to measure to a useful level of accuracy. We assume that no crystallization occurs upon compression, since there are no significant changes in the onset temperature nor in the heat of crystallization. Further FDSC characterization was carried out at a range of heating rate Φ from 20 to 10,000 K s^{-1}.

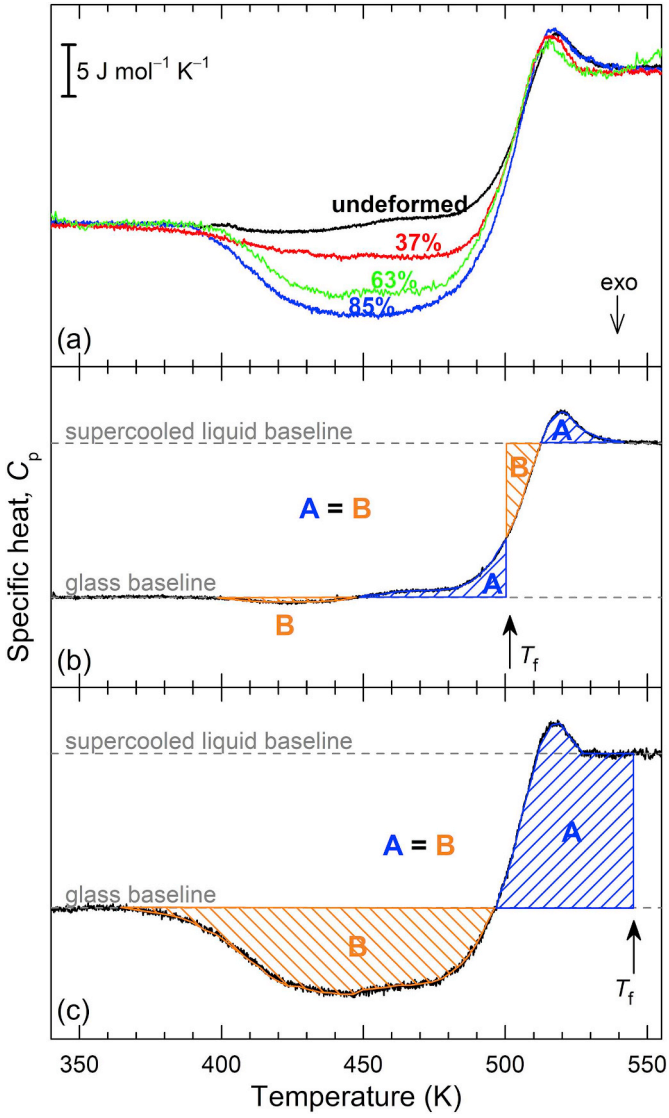

Fig. 1. (a) Specific-heat C_p curves of the $La_{55}Al_{25}Ni_{20}$ rod (aged at RT for ~1 yr) before compression ('undeformed') and after deformation (to the indicated plastic strains), focused on the structural relaxation before the glass transition, and obtained by scaling the heat-flow curves measured by FDSC at 100 K s^{-1}. **(b,c)** The equal-area construction used to determine the fictive temperature T_f, in the rod sample: (b) undeformed, and (c) compressed to 85% strain. T_f is placed so that when considering the glass transition to occur as a simple step at T_f, the area contained below the measured curve but above the horizontal line (area A) is equal to the area below the horizontal line but above the measured curve (area B).

3. Results

3.1. Increase in enthalpy after plastic deformation

A glass, when heated at a rate lower than that at which it was formed on cooling, shows structural relaxation, and in a DSC trace this appears as an exotherm below T_g. Undeformed $La_{55}Al_{25}Ni_{20}$ discs cut from a rod stored at RT for ~1 yr, show negligible relaxation on heating at 100 K s^{-1} in FDSC. After compression, a relaxation exotherm appears (Fig. 1a), and the induced rejuvenation, the difference in heat of relaxation ΔH_{rel}, is given by:

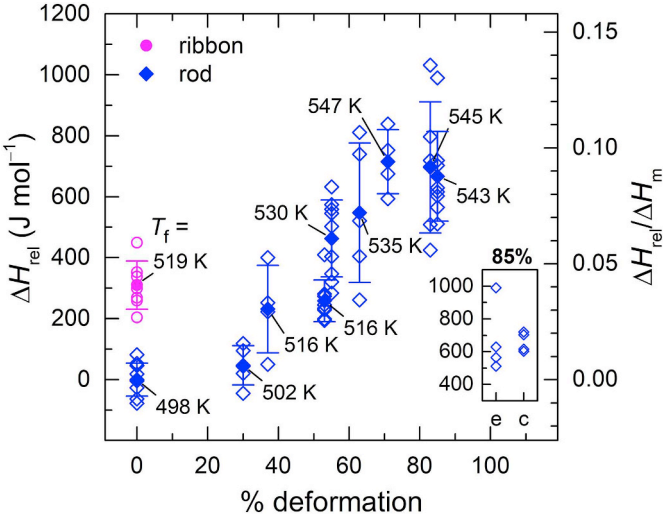

Fig. 2. The increase in energy ΔH_{rel} of the rod after compression to different degrees of deformation (diamond symbols) and of the ribbon (circle symbols). The zero point was taken as the average ΔH_{rel} of the undeformed rod. Each open symbol corresponds to a single measurement. The solid symbols and error bars correspond to the mean ± 1 standard deviation. The average fictive temperatures T_f are given by the labels. The inset shows ΔH_{rel} measured for pieces originating from the edge (e) and from the centre (c) of the sample compressed to a strain of 85%.

$$\Delta H_{rel} = \int_{T_1}^{T_2} (C_{p,init}(T) - C_{p,def}(T))dT \quad (1)$$

where $C_{p,init}(T)$ and $C_{p,def}(T)$ are the effective specific heats of the initial and deformed samples; T_1 (360 K) is below any structural relaxation and T_2 (540 K) is in the supercooled-liquid region. After a threshold of ε_p = 25–30%, ΔH_{rel} increases linearly with the plastic strain, with no indication of any saturation (Fig. 2). One can consider that increasing plastic deformation erases the prior thermal history.

Melt-spun ribbon of the same composition, also stored at RT for ~1 yr without deformation, shows a ΔH_{rel} equivalent to that in the rod compressed by 53–55%. After compression by 85%, ΔH_{rel} in the rod increases by ~667 J mol^{-1} (corresponding to ~9% of the heat of melting ΔH_m = 7.6 kJ mol^{-1} [19]). For each ε_p, the measurements of ΔH_{rel} show a wide variation, up to ± 275 J mol^{-1}, compared to ± 80 J mol^{-1} for the uncompressed samples. The inset in Fig. 2 shows that, for ε_p = 85%, the variation is significantly wider at the sample edge than in the centre, with no clear trend in average value from centre to edge.

Under the uniaxial compression in the present work, the sample spreads laterally, somewhat constrained by friction with the platens of the test machine. This constraint is not controlled and is sensitive to the nature of the sample surfaces and whether they are parallel. Thus, the variation of ΔH_{rel} values in Fig. 2 is attributed to non-uniform deformation, particularly at the edge of the samples. With the simple deformation technique and its lack of controlled constraint, this non-uniformity in deformation is difficult to reduce.

The fictive temperature T_f of the MG samples is determined using the equal-area construction [16] (Fig. 1b,c). For the calculation of effective cooling rate from T_f [8], we take the standard T_g of the MG to be 477 K (for consistency of temperature calibration, estimated from the mid-point of the glass transition in FDSC in the present work, extrapolated to Φ = 0.33 K s^{-1}) in broad agreement with published values [10,20]. We take the fragility of $La_{55}Al_{25}Ni_{20}$ liquid to be m = 33 [14,19,21], corresponding to the 'strong' liquid just above T_g [13]. The undeformed rod has T_f = 498 K, corresponding to an effective cooling rate of 8 K s^{-1}; even ~1 yr after casting, these values are higher than those of a 'standard' glass (477 K = T_g, 0.33 K s^{-1}). After deformation, the highest average T_f = 547 K corresponds to 5570 K s^{-1}. And for the ribbon T_f = 519 K corresponds to 155 K s^{-1}.

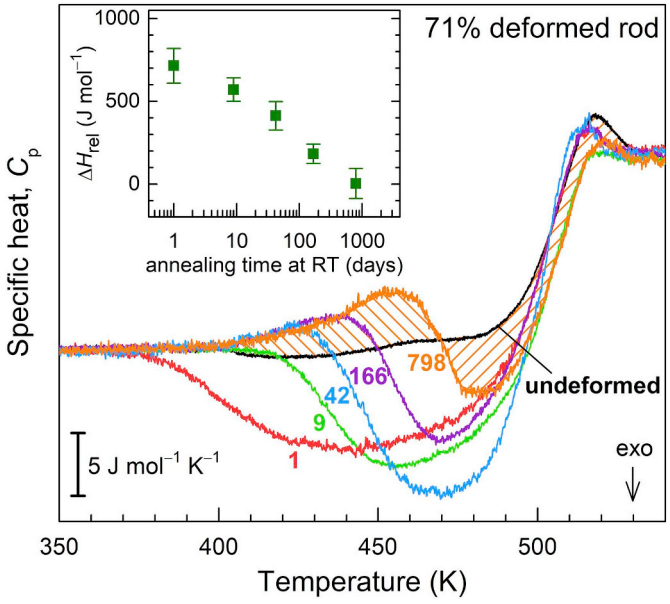

Fig. 3. Specific-heat C_p curves of the $La_{55}Al_{25}Ni_{20}$ rod (aged at RT for ~1 yr) compressed by 71% and annealed at room temperature (RT) for the indicated number of days (from 1 to 798), obtained by scaling the heat-flow curves measured by FDSC at 100 K s^{-1}. **Inset:** the effect of room-temperature (RT) annealing on the average increase in ΔH_{rel} for the rod compressed to 71% strain. The error bars show ± 1 standard deviation. ΔH_{rel} = 0 is set as the average value for the undeformed rod. ΔH_{rel} was calculated using Eq. (1) for all curves; for curves showing only a sub-T_g exotherm (e.g. after 1 day at RT), ΔH_{rel} is equal to the area of the exotherm (i.e. area between the deformed and undeformed curves). For curves showing also an endotherm (e.g. after 798 days at RT), ΔH_{rel} corresponds to the difference between the exotherm and endotherm areas (indicated by the different oblique hatching).

The actual cooling rate at T_g during casting of the MG rod is estimated to be ~300 K s^{-1} (from data in [22] with materials parameters and rod diameter adjusted for the present case). The cooling rate in melt-spinning is ~10^5–10^6 K s^{-1} [14]. For the rod, and even more for the ribbon, the effective cooling rates derived from T_f are far below the likely actual values when the MG was formed on cooling: the samples must have undergone significant relaxation during storage at RT. We next explore such ageing effects for samples freshly rejuvenated by deformation.

3.2. Room-temperature ageing after plastic deformation

For the $La_{55}Al_{25}Ni_{20}$ MG, RT corresponds to ~62% of T_g (= 477 K). The effect of RT ageing was investigated on the rod compressed by 71%. On ageing, the onset of the exotherm moves to higher temperatures (Fig. 3), and the overall heat of relaxation decreases roughly linearly with log(time) (inset). Around 2 yr after deformation, ΔH_{rel} has returned to values characteristic of the undeformed rod (which had already been aged at RT for ~1 yr).

In the FDSC trace measured 42 days after deformation, there is an endotherm at the onset of the exotherm; this is more prominent and peaks at higher temperature upon further ageing (Fig. 3). Such a sub-T_g endotherm developing upon annealing of fast-quenched glasses has been reported for MGs [13,23–28] and for oxide [15] and chalcogenide [29,30] glasses. The endotherm can be considered as a *shadow glass transition* [15], and depends on the glass being heterogeneous [31] and having a wide range of structural relaxation times. Accordingly, it is stronger for glasses formed at higher cooling rates and from liquids of higher fragility [14,30].

The effects of annealing on the stored energy in glasses have mostly

been studied using isochronal anneals at a series of temperatures [13,30]. In the present work, in contrast, we use isothermal anneals (at RT) at a series of times. Broadly, however, the effects on DSC traces on subsequent heating are the same: stronger anneals (higher temperature or longer time) cause the onset of exothermic relaxation to be shifted to higher temperature and the appearance of a sub-T_g endotherm.

The MG inherits its heterogeneity from the supercooled liquid. During quenching, slow-relaxing regions are trapped in relatively disordered states of high T_f. Fast-relaxing regions are not trapped and attain relatively ordered states of low T_f. On subsequent annealing and heating in DSC, however, these stable ordered states are slow to disorder [29]. After heating to temperatures higher than the anneal temperature, there is a sharp endotherm when these low-T_f regions do start to disorder and evolve to higher T_f. At still higher temperature, the slow-relaxing high-T_f regions resume their exothermic evolution to more ordered states of lower T_f.

Although the increase in energy due to deformation relaxes away entirely after 2 yr at RT, the sub-T_g endotherm and a compensating exotherm are still present, indicating that the combination of plastic deformation and ageing can lead to a glass of the same energy but a different structure compared to the initial state. While T_f is useful in characterizing a glass, it is far from sufficient to specify a given state.

We next use a range of Φ to investigate further the state of the glass.

3.3. Heating-rate effects on sub-T_g relaxation

A MG with higher T_f is less relaxed, but also more heterogeneous [32], with a wider spectrum of relaxation times — factors that favour the appearance of a sub-T_g endotherm. We examine the role of Φ in observing this endotherm, with FDSC permitting a wide range of rates.

The rod sample deformed by 71% has the highest T_f observed in the present work (547 K, Fig. 2). The sub-T_g endotherm is clear after ageing for 42 days at RT (Fig. 3), when heating at 100 K s^{-1}. Examining over the range 20 to 10,000 K s^{-1} (Fig. 4a) this endotherm is more evident at higher Φ. For the ribbon aged at RT for ~1 yr, examined at a range of Φ (Fig. 4b), the endotherm is also present: it is clear at 500 K s^{-1} and increases with increasing Φ until it merges with the specific-heat step at T_g. The rod aged at RT for ~1 yr has the lowest T_f in the present work. It does not show any sub-T_g endotherm until possibly at 10,000 K s^{-1} (Fig. 4c), at which rate the DSC trace near T_g is rather similar to that for the rod deformed to ε_p = 71%.

Comparison of Figs. 4a–c shows that the sub-T_g endotherm is, as expected, more evident for a glass of higher T_f. The results confirm that this is so even if the higher T_f is achieved by plastic deformation rather than by more rapid cooling from the liquid.

The peak temperature T_p of the sub-T_g endotherm is a function of Φ. The consistent trends in Fig. 4d confirm that the peaks for the ribbon and for the deformed-and-aged rod represent the same phenomenon. Compared to the ribbon, the T_p values are lower for the deformed-and-aged rod, consistent with it being less relaxed (with ΔH_{rel} ~ 100 J mol^{-1} higher than for the ribbon). A linear fitting of these Kissinger plots gives an effective activation energy E_a = 101 ± 4 kJ mol^{-1} for both the ribbon and the deformed-and-aged rod, matching the activation energy of the β relaxation for this composition (100–110 kJ mol^{-1} [10,14]). Furthermore, $E_a \approx 26 (\pm 1) RT_g$, where R is the gas constant, fitting perfectly the accepted correlation between the activation energy of the β relaxation and T_g [12,14]. Similar agreement between the activation energies for the sub-T_g endotherm and the β relaxation has been observed also for a Au-based MG [26], and for Zr-based and La-based MGs [33]. The endotherm indicates the kinetic unfreezing, by thermal activation, of β relaxation on heating [26,33]. The activation energy could alternatively be determined using a plot of log(Φ) vs $1/T_p$ [26]; in practice the value of E_a is barely affected by this change from the Kissinger plot.

For $La_{55}Al_{25}Ni_{20}$ ribbons annealed at selected temperatures in the range 343–493 K for 30 min, DSC traces on heating at 0.333 K s^{-1} show no endotherm [14]. Comparing glasses in general, and MGs in particular, Hu and Yue concluded that the sub-T_g endotherm is absent in glasses such as $La_{55}Al_{25}Ni_{20}$ formed from stronger liquids [14,21]. While it is clear that the endotherm is weaker in such glasses, the present results show that the endotherm is detectable for $La_{55}Al_{25}Ni_{20}$, after annealing at a lower temperature for longer times and on heating at the considerably higher rates achievable by FDSC.

3.4. Excess exotherm

In the many reports of the sub-T_g endotherm in MGs and other glasses, on heating beyond the endotherm the DSC traces generally converge on to the trace of an unannealed sample. In contrast, in Fig. 3, the traces clearly cross over each other rather than converging monotonically. The trace for a sample annealed at RT for 42 days, shows a clear *excess exotherm* at ~470 K. The exotherm is strongest for intermediate annealing times. The exotherm can be considered as an overshoot effect (§4.3) in which ordering is delayed and therefore must be faster. The effect increases with annealing time until the delayed ordering starts to overlap with the glass transition.

An excess exotherm can be seen in reported data [10,13,30]; it is usually weak, but is very clear in CDSC traces of annealed GeO_2 glass [14] for which the liquid is strong (m = 18). But in no case has there been comment on this excess-exothermic (i.e. ordering) effect.

4. Discussion

4.1. Stored energy

For polycrystalline metals, the stored energy after plastic deformation at RT is 1–10% of the mechanical work done (WD) [34], and this fraction seems to be similar for MGs. Chen originally found that the stored energy is ~4% of WD [3], and later typical values from the literature on MGs, surveyed in Table 1, range from 1.5 to 6%. By reducing the height:diameter aspect ratio, high ε_p can be achieved even in simple uniaxial compression of MGs. For example, Zr-based BMG rods of aspect ratio < 0.5–1 can be compressed at low strain rates of order 10^{-4} s^{-1} to ε_p = 46–80% without fracture [35–37], leading to a decrease in hardness of as much as ~15% [35], and increased compressive plasticity [36]; even so, the increase of ΔH_{rel} is still ~4% of the WD [37].

For deformation at lower temperature, this fraction can be increased, for example to 10% at 150 K [2] and 16% at 77 K [39].

In the present work, for the rod compressed to ε_p = 55%, the increase in ΔH_{rel} corresponds to ~3% of the work done; while this is in the range of values expected for MGs, it may be unusually high for deformation at a temperature (RT) that is 62% of T_g.

For uniaxial compression of simple (unnotched) samples, even the highest stored energies (as a fraction of the WD at RT) are far below the 29% achieved in notched BMG rods [8]. While there is some degree of triaxial constraint in compression of samples of low aspect ratio, it seems that this is not sufficient to suppress relaxation during deformation and to achieve the high ratio of (stored energy)/(work done) found at the centre of notched samples subjected to compression.

4.2. Relaxation spectrum

In addition to the area of the relaxation exotherm, its shape (the *relaxation spectrum* [3]) can provide information on the effect of deformation. When heating as-cast MGs at conventional rates (e.g. 0.33 K s^{-1}), structural relaxation starts at ~0.6 T_g and continues up to T_g. The relaxation spectrum shows a variety of shapes [40], sometimes monomodal with its maximum close to T_g, sometimes bimodal with an excess shoulder or even a separate peak at lower temperatures, which is considered as the β relaxation whereas the main peak closer to T_g corresponds to the α relaxation.

Plastic deformation can decrease the onset temperature T_{rel} of the

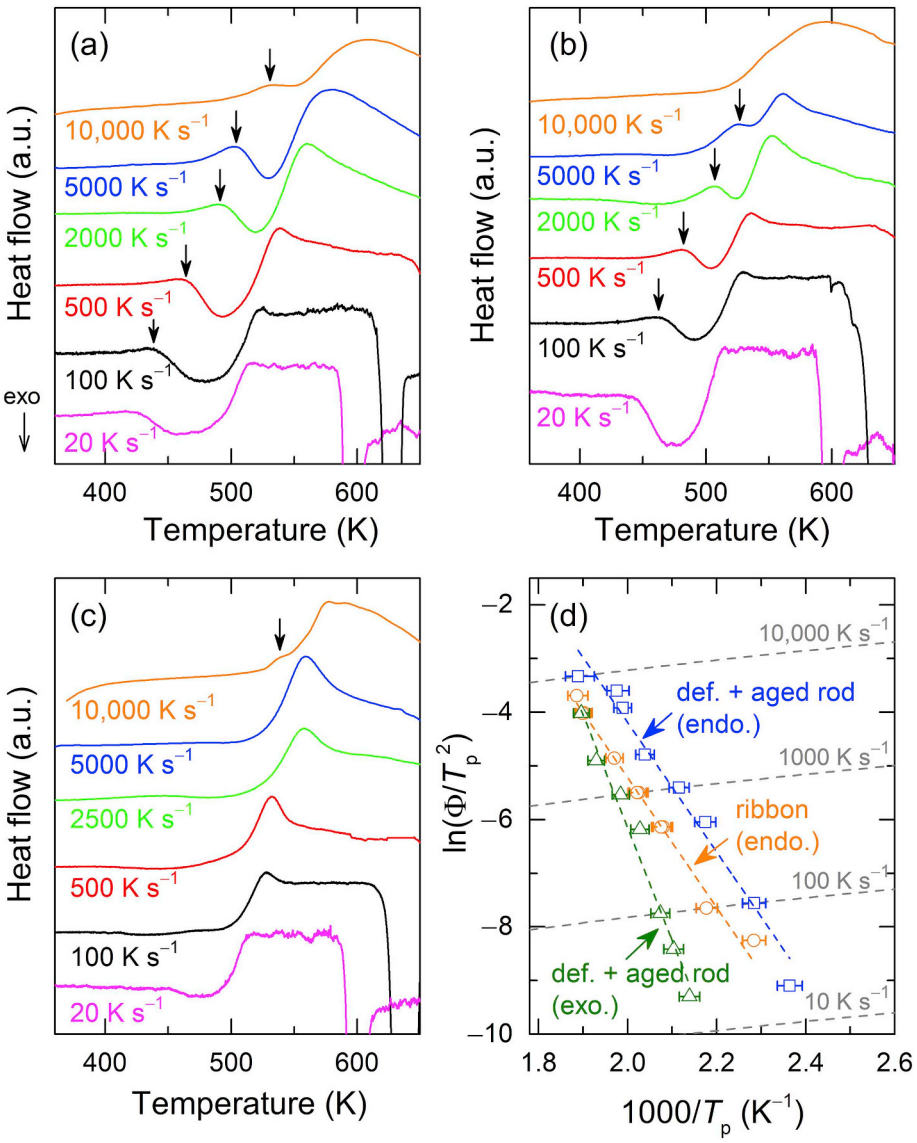

Fig. 4. Example FDSC traces for $La_{55}Al_{25}Ni_{20}$ MG (aged at RT for ~1 yr), focusing on the endothermic sub-T_g peak (indicated by the arrows) at different heating rates Φ: (a) for rod deformed by 71% and aged for 42 days at RT; (b) for melt-spun ribbon; and (c) for undeformed rod. The heat-flow curves are scaled to facilitate comparison at different Φ. (d) Kissinger plot showing the peak temperature T_p of the sub-T_g endotherm at different Φ for the melt-spun ribbon, and the endotherm and excess exotherm for the 71% deformed rod aged at RT for 42 days. The activation energy of the sub-T_g peak is estimated from a linear fitting (orange and blue dashed lines) of these points. (For interpretation of the references to colour in this figure legend, the reader is referred to the web version of this article.)

relaxation spectrum [2,38,41], promote the growth of the β peak [38,39,41], and increase the main peak height [2,3,39]. The onset of relaxation at T_{rel} has been tentatively associated with atomic-size voids, the β relaxation with free volume in flow defects and shear bands, and the α relaxation with free volume in the dense glass [40].

Although the undeformed La-based rod measured here shows overall negligible structural relaxation, there is a hint of a bimodal exotherm, with a first maximum at ~425 K and a second at ~480 K (Fig. 1a). This bimodal shape persists after compression to 63%, but on further deformation, the spectrum is monomodal. The value of T_{rel} for the undeformed rod, 386 K (~0.80 T_g), is barely changed by deformation, decreasing to ~0.76 T_g at 85% strain, but this change is within the variation measured for different samples deformed to a given strain. This T_{rel} is a higher fraction of T_g than for other MG compositions after plastic deformation: e.g. cold-rolling of a Ni-based MG decreased T_{rel} from 0.72 to 0.54 T_g [41] and shot-peening of a Pd-based MG decreased T_{rel} from 0.60 to 0.55 T_g [38].

As seen in Section 3.2, the higher and relatively fixed value of T_{rel}/T_g in the present work can be understood to result from RT ageing in the time between deformation and FDSC measurement. For the same composition, ribbon samples heated in CDSC within 1 h after melt-spinning, showed T_{rel} as low as ~340 K (= 0.7 T_g) [10]. The RT ageing in the present work must reduce the β-relaxation peak in particular, and thus is likely to have reduced any bimodal character of the relaxation spectra.

That RT ageing can affect measurements of stored energy arising from deformation has previously been reported for a Au-based BMG [42], but that work compared only two ageing times, up to 2 months.

4.3. Rejuvenation reversed by RT ageing

The RT ageing noted in §3.1 was first demonstrated for melt-spun ribbons of $La_{55}Al_{25}Ni_{20}$ by Okumura et al. [10]. Using their conventional DSC data (Fig. 2 in [10]), we calculate (as in §3.1, using the method outlined by Pan et al. [8]) that the ribbon measured 1 h after quenching has T_f = 559 K and an effective cooling rate of ~23,000 K s^{-1}, and measured 2 months after has T_f = 533 K and an effective rate of ~1000 K s^{-1}. Hu and Yue report that 'fresh' quenched ribbon of the same composition has an enthalpy 1.2–1.4 kJ mol^{-1} higher than a standard glass; from this value we calculate that the sample has T_f = 577 K and an effective cooling rate of ~174,000 K s^{-1}.

Fig. 5 plots these values of T_f and that for the ribbon (aged for ~1 yr at RT) in the present work. The decay of T_f is compared with the data for the deformed-and-aged rod (Fig. 3). Despite the approximate time-values for the ribbon samples, a consistent pattern emerges. For the ribbon samples and for the rod, the relaxation (ageing) is initially very

Table 1
Examples of enthalpy increases induced in metallic glasses by various methods of plastic deformation. Estimates are given of the percentage of mechanical work done that these energy increases represent.

Process	Details	Enthalpy increase (J mol^{-1})	% of work done
Cold-rolling	36% thickness reduction of a Pd-based ribbon [3]	200	4%[a]
	90% thickness reduction of a Cu-based BMG [2]	820 (rolled at RT)	6%[b]
		1350 (rolled at 150 K)	10%[b]
High-pressure torsion	50 rotations (peripheral strain = 925) applied to a Zr-based BMG disc [4]	1770	4%[c]
Shot-peening	30 s peening of a Pd-based BMG [38]	85[d]	5.7%[a]
	60 s peening of a pre-annealed Pd-based BMG rod [39]	152[d] (peened at RT)	5%[e]
		468[d] (peened at 77 K)	16%[e]
Uniaxial compression of a 2:1-aspect-ratio sample	40% strain of a Zr-based BMG rod [8]	160	1.5%[a]
Triaxial compression	40% strain at the notch in a Zr-based BMG rod [8]	640[f]	29%[a]
		2930[g]	–
Compression of low-aspect-ratio sample	68% strain, Zr-based BMG rod [37]	552	4%[a]
	Present work on La-based BMG rod:		
	37% strain	230	–
	55%	500	3%[b]
	85%	670	–

[a] Given in the corresponding reference.
[b] Estimated in the present work using the method in [3].
[c] Estimated in the present work, using the known flow stress and averaging over the area of the disc.
[d] For a peened surface layer of 150 μm depth.
[e] Estimated in the present work using the method in [38].
[f] Measured over the full disc defined by the circumferential notch.
[g] Measured at the perimeter of the notched disc.

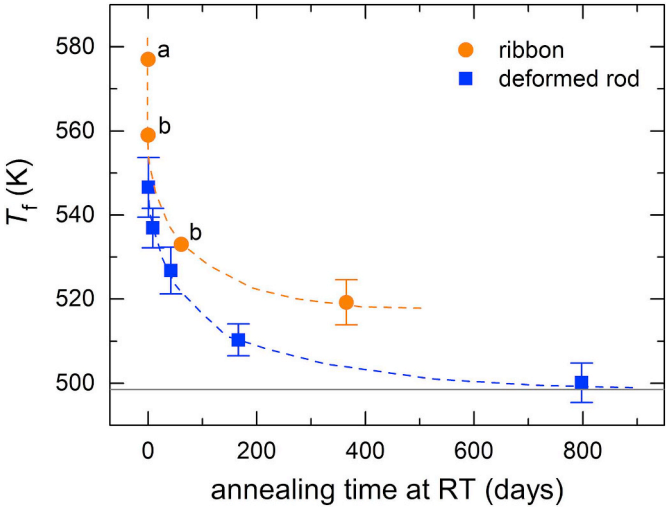

Fig. 5. Effect of room-temperature (RT) annealing on the fictive temperature T_f of $La_{55}Al_{25}Ni_{20}$ ribbon and of the rod deformed by 71%; the dashed lines show the trend of decay. The horizontal line at T_f = 498 K represents the average value of T_f for the undeformed rod (aged at RT for ~1 yr). The points denoted by (a) and (b) were estimated by us using conventional DSC data from [10,14], respectively. The error bars represent ± 1 standard deviation.

rapid and then slows, consistent with the log(time)-dependence of ΔH_{rel} in Fig. 3 (inset). The freshly quenched ribbon and deformed rod can both be regarded as *rejuvenated*, but their T_f values do not converge at long times as would be the case if the rate of relaxation depends only on the value of T_f. Rather, for a given T_f, the deformed rod relaxes much faster, and within the period shown returns to the value for the undeformed rod.

The compressed rod in the present work has deformed by shear-banding, and thus the structure (and local effective values of T_f) must be heterogeneous. The data in Fig. 5 show that the most rejuvenated regions must undergo particularly rapid ageing, consistent with the high value of T_{rel} discussed in §4.2. We conclude that deformation-induced rejuvenation of a MG (at least when deformation is by the usual shear-banding) is particularly susceptible to reversal by annealing, as shown in the present case by ageing at RT. Nevertheless, as noted in §3.2, although the stored energy of deformation can be completely removed by RT ageing, the sample does not return to its previous structure. There is thus the possibility that some of the effects of the deformation on (for example) mechanical properties can be retained.

4.4. Overshoot effects

When a glass is heated faster than the cooling rate to which its T_f conforms, there is an endothermic overshoot on the high-temperature side of the glass transition. In effect, the rapid heating causes the degree of disordering at a given temperature to lag, requiring a catch-up at higher temperature. For a given T_f, this effect is obviously greater for higher Φ. Analogously, for a given Φ, the effect is greater for lower T_f. The sub-T_g endotherm, or shadow glass transition, reflects a similar overshoot effect for local regions of high order (low T_f) rather than for the glass as a whole. As a result of annealing at a temperature well below T_g, these regions are trapped for longer in their low-T_f states and subsequent rapid disordering gives the endotherm.

Annealing well below T_g enables relaxation towards lower T_f and removes the lower-temperature portion of the relaxation spectrum. But the excess exotherm observed in the present work (§3.4) suggests that the annealing can also lead to local regions being trapped for longer in their high-T_f states; this leads to an overshoot effect analogous to, but of opposite sign to, the sub-T_g endotherm.

It has been noted that the sub-T_g endotherm, observable by DSC after hyperquenching and annealing, provides valuable information on β-relaxation dynamics in glasses in general and MGs in particular [14]. We suggest that the excess exotherm (Fig. 3) is similarly useful. The role of Φ in studying these effects is shown in Fig. 6. This compares the FDSC traces for $La_{55}Al_{25}Ni_{20}$ MG rod aged for ~1 yr at RT with the same rod compressed to ε_p = 71% and then aged at RT for 42 days. The sub-T_g endotherm (identified by the arrows in Fig. 4a for the deformed sample) is stronger (and at higher temperature) for higher Φ. It is also clear that the relaxation exotherm in the deformed sample is displaced to higher temperature (relative to the glass transition) at higher Φ, thus facilitating observation of the excess exotherm identified in the present work. Taking the peak temperature of the exotherm in Fig. 6, its variation with Φ (plotted in Fig. 4d) gives an effective activation energy, 175 ± 11 J mol^{-1}, that is intermediate between that of the β relaxation and that of the glass transition (α relaxation). The range of

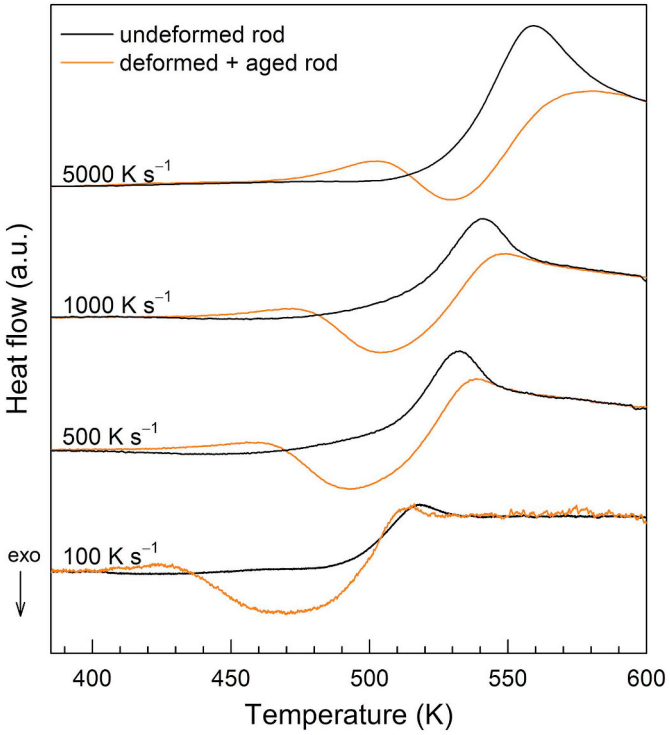

Fig. 6. Example FDSC traces of the undeformed $La_{55}Al_{25}Ni_{20}$ MG rod (aged for ~1 yr at RT) and of the rod deformed by 71% and aged for 42 days at RT, measured at different heating rates. The heat-flow curves are scaled for easier comparison.

behaviour in Fig. 6 gives opportunities for further analysis of relaxation dynamics.

5. Conclusions

Samples of $La_{55}Al_{25}Ni_{20}$ metallic glass (2 mm diameter rod and melt-spun ribbon) were studied after storage at RT for ~1 yr. Sliced from the rod, discs with low aspect ratio (height/diameter < 0.4) were compressed normal to their faces. The low aspect ratio of the samples permits high plastic strains, up to 85%, to be achieved. The enthalpy of the glass increased by up to ~700 J mol^{-1}, representing a stored energy that is ~3% of the mechanical work done. Despite the degree of triaxial constraint due to the low aspect ratio, this stored-energy fraction remains at the usual low level, and does not reach the tenfold higher level seen with the greater constraint in axial compression of notched rods.

Room temperature is 62% of the glass-transition temperature for this glass. As a result there is significant structural relaxation at RT: the stored energy of deformation decreases roughly linearly with log(time) and reaches zero after ~2 yr. Differential scanning calorimetry shows that the deformed-and-aged sample is not the same as before deformation, however, confirming that the fictive temperature is insufficient to characterize the state of the glass, and leaving open the possibility that despite the ageing there can be longer-lasting effects of the deformation.

The relaxation of the deformed sample is much faster at a given fictive temperature than in an undeformed melt-spun ribbon: the stored energy induced by heterogeneous deformation (mediated by shear-banding) is more easily reduced by subsequent ageing.

Fast FDSC traces on heating the deformed rod after intermediate ageing times show a sub-T_g endotherm before the relaxation exotherm. This endotherm has been widely studied, but was thought to be absent for the MG in this work. We show that it becomes measurable at the high heating rates obtainable using FDSC and is associated with β relaxation. The endotherm is readily detectable also for the melt-spun ribbon, and just detectable for the undeformed rod at the highest heating rate.

After intermediate ageing times, FDSC traces on heating also show, after the endotherm, an excess exotherm. This has been seen in earlier work, but not noted. We suggest that this exotherm is an overshoot effect analogous to the sub-T_g endotherm, both arising at high heating rate. The endotherm appears favoured in systems where the liquid has a high fragility, and the exotherm conversely with low fragility.

The present results show that, even for well annealed samples, mechanical deformation is effective in raising the stored energy in MGs to values characteristic of rapid quenching. Deformation increases the heterogeneity of the glass, widening the spectrum of relaxation times. The high heating rates in FDSC are helpful in revealing new relaxation phenomena such as the excess exotherm.

Disclosure statement

No potential conflict of interest was reported by the authors.

Declaration of Competing Interest

The authors declare that they have no known competing financial interests or personal relationships that could have appeared to influence the work reported in this paper.

Acknowledgements

The authors are grateful for the provision of the MG samples by W.-H. Wang. This work was supported by the European Commission, Marie Skłodowska-Curie Actions, grant FP7-PEOPLE-2013-ITN-607080, 'VitriMetTech' (for CMM), and by the European Research Council, grant ERC-2015-AdG-695487, 'ExtendGlass' (for JO and ALG).

References

[1] Y. Sun, A. Concustell, A.L. Greer, Thermomechanical processing of metallic glasses: extending the range of the glassy state, Nat. Rev. Mater. 1 (2016) 16039.
[2] Q.P. Cao, J.F. Li, Y.H. Zhou, A. Horsewell, J.Z. Jiang, Free-volume evolution and its temperature dependence during rolling of $Cu_{60}Zr_{20}Ti_{20}$ bulk metallic glass, Appl. Phys. Lett. 87 (2005) 101901.
[3] H.S. Chen, Stored energy in a cold-rolled metallic glass, Appl. Phys. Lett. 29 (1976) 328–330.
[4] F. Meng, K. Tsuchiya, S. Il, Y. Yokoyama, Reversible transition of deformation mode by structural rejuvenation and relaxation in bulk metallic glass, Appl. Phys. Lett. 101 (2012) 121914.
[5] O.A. Hasan, M.C. Boyce, Energy storage during inelastic deformation of glassy polymers, Polymer 34 (1993) 5085–5092.
[6] A.L. Greer, Y.Q. Cheng, E. Ma, Shear bands in metallic glasses, Mater. Sci. Eng. R 74 (2013) 71–132.
[7] S. Balachandran, J. Orava, M. Köhler, A.J. Breen, I. Kaban, D. Raabe, M. Herbig, Elemental re-distribution inside shear bands revealed by correlative atom-probe tomography and electron microscopy in a deformed metallic glass, Scr. Mater. 168 (2019) 14–18.
[8] J. Pan, Y.X. Wang, Q. Guo, D. Zhang, A.L. Greer, Y. Li, Extreme rejuvenation and softening in a bulk metallic glass, Nat. Commun. 9 (2018) 560.
[9] S.V. Ketov, Y.H. Sun, S. Nachum, Z. Lu, A. Checchi, A.R. Beraldin, H.Y. Bai, W.H. Wang, D.V. Louzguine-Luzgin, M.A. Carpenter, A.L. Greer, Rejuvenation of metallic glasses by non-affine thermal strain, Nature 524 (2015) 200–203.
[10] H. Okumura, H.S. Chen, A. Inoue, T. Masumoto, Sub-T_g mechanical relaxation of a $La_{55}Al_{25}Ni_{20}$ amorphous alloy, J. Non-Cryst. Solids 130 (1991) 304–310.
[11] W.H. Wang, Dynamic relaxations and relaxation-property relationships in metallic glasses, Prog. Mater. Sci. 106 (2019) 100561.
[12] H.B. Yu, W.H. Wang, K. Samwer, The β relaxation in metallic glasses: an overview, Mater. Today 16 (2013) 183–191.
[13] L. Hu, C. Zhou, C. Zhang, Y. Yue, Thermodynamic anomaly of the sub-T_g relaxation in hyperquenched metallic glasses, J. Chem. Phys. 138 (2013) 174508.
[14] L. Hu, Y. Yue, Secondary relaxation in metallic glass formers: its correlation with the genuine Johari-Goldstein relaxation, J. Phys. Chem. C 113 (2009) 15001–15006.
[15] Y. Yue, C.A. Angell, Clarifying the glass-transition behaviour of water by comparison with hyperquenched inorganic glasses, Nature 427 (2004) 717–720.
[16] C.T. Moynihan, A.J. Easteal, M.A. DeBolt, J. Tucker, Dependence of the fictive temperature of glass on cooling rate, J. Am. Ceram. Soc. 59 (1976) 12–16.
[17] A.L. Greer, J.A. Leake, Structural relaxation and crossover effect in a metallic glass, J. Non-Cryst. Solids 33 (1979) 291–297.

[18] Z.P. Lu, Y. Li, C.T. Liu, Glass-forming tendency of bulk La–Al–Ni–Cu–(Co) metallic glass-forming liquids, J. Appl. Phys. 93 (2003) 286–290.
[19] R. Jia, X.F. Bian, Y.Y. Wang, Thermodynamic determination of fragility in La-based glass-forming liquid, Chin. Sci. Bull. 56 (2011) 3912–3918.
[20] Z.P. Lu, T.T. Goh, Y. Li, S.C. Ng, Glass formation in La-based La-Al-Ni-Cu-(Co) alloys by Bridgman solidification and their glass forming ability, Acta Mater. 47 (1999) 2215–2224.
[21] Y. Kawamura, T. Nakamura, H. Kato, H. Mano, A. Inoue, Newtonian and non-Newtonian viscosity of supercooled liquid in metallic glasses, Mater. Sci. Eng. A 304–306 (2001) 674–678.
[22] T. Koziel, Estimation of cooling rates in suction casting and copper-mould casting processes, Arch. Metall. Mater. 60 (2015) 767–771.
[23] H.S. Chen, On mechanisms of structural relaxation in a $Pd_{48}Ni_{32}P_{20}$ glass, J. Non-Cryst. Solids 46 (1981) 289–305.
[24] H.S. Chen, Kinetics of low temperature structural relaxation in two (Fe-Ni)-based metallic glasses, J. Appl. Phys. 52 (1981) 1868–1870.
[25] H.S. Chen, A. Inoue, Sub-T_g enthalpy relaxation in PdNiSi alloy glasses, J. Non-Cryst. Solids 61&62 (1984) 805–810.
[26] Z. Evenson, S.E. Naleway, S. Wei, O. Gross, J.J. Kruzic, I. Gallino, W. Possart, M. Stommel, R. Busch, β relaxation and low-temperature aging in a Au-based bulk metallic glass: From elastic properties to atomic-scale structure, Phys. Rev. B 89 (2014) 174204.
[27] A. Inoue, T. Masumoto, H.S. Chen, Enthalpy relaxation behaviour of (Fe, Co, $Ni)_{75}Si_{10}B_{15}$ amorphous alloys upon low temperature annealing, J. Mater. Sci. 19 (1984) 3953–3966.
[28] P.T. Vianco, J.C.M. Li, Analysis of the endothermic peak in an annealed metallic glass, J. Non-Cryst. Solids 107 (1989) 225–232.
[29] O. Gulbiten, J.C. Mauro, P. Lucas, Relaxation of enthalpy fluctuations during sub-T_g annealing of glassy selenium, J. Chem. Phys. 138 (2013) 244504.
[30] J. Pries, S. Wei, M. Wuttig, P. Lucas, Switching between crystallization from the glassy and the undercooled liquid phase in phase change material $Ge_2Sb_2Te_5$, Adv. Mater. 31 (2019) 1900784.
[31] C. Liu, R. Maaß, Elastic fluctuations and structural heterogeneities in metallic glasses, Adv. Funct. Mater. 28 (2018) 1800388.
[32] K B Kim, X F Zhang, S Yi, M H Lee, J Das, J Eckert, Effect of local chemistry, structure and length scale of heterogeneities on the mechanical properties of a Ti45Cu40Ni7.5Zr5Sn2.5 bulk metallic glass, Philos. Mag. Lett. 88 (2008) 75–81.
[33] R. Zhao, H.Y. Jiang, P. Luo, L.Q. Shen, P. Wen, Y.H. Sun, H.Y. Bai, W.H. Wang, Reversible and irreversible β-relaxations in metallic glasses, Phys. Rev. B 101 (2020) 094203.
[34] M.B. Bever, D.L. Holt, A.L. Titchener, The stored energy of cold work, Prog. Mater. Sci. 17 (1972) 5–177.
[35] H. Bei, S. Xie, E.P. George, Softening caused by profuse shear banding in a bulk metallic glass, Phys. Rev. Lett. 96 (2006) 105503.
[36] L. He, M.B. Zhong, Z.H. Han, Q. Zhao, F. Jiang, J. Sun, Orientation effect of pre-introduced shear bands in a bulk-metallic glass on its “work-ductilising”, Mater. Sci. Eng. A 496 (2008) 285–290.
[37] D.V. Louzguine-Luzgin, S.V. Ketov, Z. Wang, M.J. Miyama, A.A. Tsarkov, A.Y. Churyumov, Plastic deformation studies of Zr-based bulk metallic glassy samples with a low aspect ratio, Mater. Sci. Eng. A 616 (2014) 288–296.
[38] F.O. Méar, B. Lenk, Y. Zhang, A.L. Greer, Structural relaxation in heavily cold-worked metallic glass, Scr. Mater. 59 (2008) 1243–1246.
[39] A. Concustell, F.O. Méar, S. Suriñach, M.D. Baró, A.L. Greer, Structural relaxation and rejuvenation in a metallic glass induced by shot-peening, Philos. Mag. Lett. 89 (2009) 831–840.
[40] A.L. Greer, Y.H. Sun, Stored energy in metallic glasses due to strains within the elastic limit, Philos. Mag. 96 (2016) 1643–1663.
[41] B. Jessen, E. Woldt, Stored energy of the deformed metallic glass $Ni_{78}Si_8B_{14}$, Thermochim. Acta 151 (1989) 179–186.
[42] X.D. Wang, Q.P. Cao, J.Z. Jiang, H. Franz, J. Schroers, R.Z. Valiev, Y. Ivanisenko, H. Gleiter, H.-J. Fecht, Atomic-level structural modifications induced by severe plastic shear deformation in bulk metallic glasses, Scr. Mater. 64 (2011) 81–84.